

Reversing Degradation: Recovery of Ion-Induced Performance Losses in Perovskite Solar Cells

Paria Forozi Sowmeeh^a, Jarla Thiesbrummel^{a,b}, Andres Felipe Castro Mendez^a, Sahil Shah^c, Biruk Alebachew Seid^a, Francisco Peña-Camargo^d, Thomas Hultsch^a, Jan Hagenberg^a, Martin Stolterfoht^e, Felix Lang^a **

^a Institute of Physics and Astronomy University of Potsdam, Potsdam-Golm, Germany

^b Humboldt University Berlin, Germany

^c University of Queensland, Australia

^d Helmholtz-Zentrum Berlin für Materialien und Energie, Berlin, Germany

^e Electronic Engineering Department, The Chinese University of Hong Kong, Hong Kong SAR, China

*Corresponding Authors: felix.lang1@uni-potsdam.de, jarla.thiesbrummel.2@uni-potsdam.de

Device Fabrication

Substrate and HTL preparation: Pre-patterned ITO substrates were pre-patterned glass/ITO substrates were sonicated for 2 minutes in Acetone, prior to 2 minutes in 3% Hellmanex solution, 2×2 minutes in deionized (DI) water, and 10 minutes in acetone and iso-propanol. After sonication, the substrates were dried with a nitrogen gun prior to 4 minutes of plasma treatment. Samples were immediately transferred to a N₂-filled glovebox.

For 1.63eV sample, 60 μL PTAA (Sigma-Aldrich) layer was static spin coated from a 1.75 mg mL⁻¹ PTAA/toluene solution at 6000 rpm for 30 seconds. After 10 min annealing at 100 °C, the films were cooled down to room temperature and a 60 μL solution of PFN-Br (0.5 mg/mL in methanol) was deposited onto PTAA at 4000 rpm for 30 s without any further annealing.

For 1.58 eV samples, the same cleaning procedure was applied with the exception of using UV-ozone cleaner for 30 minutes before transferring to the N₂-filled glovebox. MeO-2PACz layer was spin-coated from a 1 mmol mL⁻¹ ethanol solution at 3000 rpm for 30 seconds and annealed at 100°C for 10 minutes.

Perovskite Cs_{0.05}(FA_{0.83}MA_{0.17})_{0.95}Pb(I_{0.83}Br_{0.17})₃ film fabrication: The 1.63eV perovskite solution was prepared by mixing two 1.2 M FAPbI₃ and MAPbBr₃ perovskite solutions in DMF:DMSO (4:1 volume ratio) in a ratio of 83:17 for FAPbI₃:MAPbBr₃. The 1.2 M FAPbI₃ solution was thereby prepared by dissolving FAI (515.9 mg) and PbI₂ (1521.3 mg) in 2 mL DMF and 0.5 mL DMSO. The MAPbBr₃ solution was made by dissolving MABr (201.5mg) and PbBr₂ (726.7 mg) in 1.2 mL DMF and 0.3 mL DMSO.

After overnight mixing at room temperature 830 μL of FAPbI₃ and 170 μL of MAPbBr₃ and 42 μL CsI solution in DMSO (389 mg CsI in μ 1 mL DMSO) were mixed.

The perovskite films were deposited by spin-coating at 4000 rpm for 40 s and 12 s after the start of the spinning process, 300 μL ethylacetate were dripped on the center of the films leading to a shiny brown color of the films. The perovskite film was then annealed at 100 °C for 1 h on a hotplate.

Perovskite Cs_{0.05}(FA_{0.95}MA_{0.05})_{0.95}Pb (I_{0.95}Br_{0.05}Cl)₃ film fabrication: The perovskite precursor solution was prepared based on the method reported by Seid et al.¹ In brief, PbI₂ (1797.94 mg), PbBr₂ (578.06 mg), MABr (79.96 mg), and FAI (567.98 mg) were dissolved in a DMF/DMSO (4:1) mixture and stirred to obtain a 1.5 M solution containing FAPbI₃ and

MAPbBr₃. Afterwards, a CsI (1.5 M) solution and MAI (20 mol%) in DMSO were added to the solution.

The 1.58eV perovskite solution was spin-coated at 4000 rpm for 40 seconds, prior to washing the film with 300 μ L of chlorobenzene 7 s prior to the end of the spin-coating process, followed by annealing the perovskite film at 100 °C for 1 hour.

ETL and top contact: After annealing, the films were transferred to the evaporator, where C60 (30 nm), 2,9-Dimethyl-4,7-diphenyl-1,10-phenanthroline BCP (8 nm), and copper (100 nm) were deposited under vacuum. Finally, the active area of 0.0648 cm² was achieved.

Device Characterizations

Current density-voltage characteristics: J-V characteristics were recorded using a 2-wire source-sense Setup with a Keithley 2400. Illumination was provided by an Oriel class AAA Xenon lamp-based sun simulator at 100 mW cm⁻² under AM1.5G conditions, while the intensity was monitored continuously with a Si photodiode. The measured illumination intensity was used for efficiency calculations. The simulator was calibrated with a KG5 filtered silicon reference solar cell (certified by Fraunhofer ISE). During the measurement, the temperature of the cell was maintained to 25 °C.

External quantum efficiency (EQE) measurements: EQE was measured as a function of wavelength with a step of 5 nm using a custom-built small spot EQE system, where the illumination beam size was 0.5 mm², smaller than the device active area (~0.0648cm²)².

Grazing-incidence XRD (GIXRD) measurements: Grazing-incidence X-ray diffraction measurements were performed using a PANalytical EMPYREAN diffractometer with Cu K α radiation ($\lambda = 1.5406 \text{ \AA}$), operated at 40 kV and 40 mA, over a 2θ range of 2–52° with a step size of 0.03° and a fixed incidence angle $\omega=3^\circ$.

In-situ Grazing-incidence XRD (GIXRD) measurements: In-situ XRD measurements were carried out using a PANalytical EMPYREAN diffractometer with a Cu anode (K $\alpha_1 = 1.5406 \text{ \AA}$, K $\alpha_2 = 1.5444 \text{ \AA}$) operated at 40 kV and 40 mA. Data were collected in continuous 2θ mode over the range 27.5°–33.5° with a step size of 0.03° and a fixed 0.19 mm divergence slit. GIXRD with a fixed incidence angle $\omega=1.0^\circ$ were performed to probe the structural evolution of the perovskite layer during illumination and the subsequent dark recovery. XRD pattern

from $2\theta = 27^\circ$ to 31.8° was measured every 10 minutes under 1 hour of illumination and 1 hour of dark resting. Prior to measurement, samples were stored in a N_2 -filled glovebox and mounted in an airtight sample holder equipped with a Kapton foil window. The holder allows X-rays to pass through while maintaining an inert environment. The sample was sealed inside the holder in the glovebox, and during measurement, a nitrogen flow was established through the holder using two valves to ensure continuous inert conditions.

For aging experiments, a white LED light source (ledxon 9009386) was used, with illumination passing through the Kapton foil before reaching the sample. The light intensity was calibrated to one sun using a reference cell at the same distance, with calibration performed without the Kapton foil. The Kapton foil shows high transmittance above 500 nm, comparable to BK7 glass, but strongly absorbs light below 500 nm.

Fast Hysteresis (FH) Measurements: Fast J-V measurements were performed by applying voltage pulses to the solar cells, starting close to the open-circuit voltage (V_{oc}). The pulse sequence consisted of a reverse scan from V_{oc} to -0.1 V, followed by a forward scan back to V_{oc} , carried out at different scan rates ($V s^{-1}$), using instrumentation provided by SolarSense Technologies Ltd. The dwell time at V_{oc} was set to be five times longer than the total sweep duration.

The voltage response was monitored with an oscilloscope while using an external load resistance of $\leq 10 \Omega$. The voltage pulses were generated with a function generator. Although the setup differed from J-V setups, the experimental conditions were consistent with those described previously. For temperature-dependent fast hysteresis (T(FH)) the temperature of the device under investigation was set to desired value using a temperature controller while conducting the fast J-Vs. Full description of the T(FH) can be found in Forozi Sowmeh et al.

3

BACE Measurements: For dark BACE measurements, the device was first biased close to its open-circuit voltage, where the injected charge compensates the short-circuit current. After a set delay, typically about five times longer than the charge extraction time under collection conditions, a bias of 0 V was applied to extract both injected and capacitive charges. This delay ensured sufficient ionic redistribution within the active layer. The resulting current transients were obtained using a Keithley 2400 source meter with a custom LabVIEW interface. The extracted charge was obtained by integrating the transient current, and the corresponding

charge carrier density was calculated by dividing the total charge by the elementary charge and the device volume.

Stabilized maximum power point (SPO) tracking: SPO tracking was performed in an ambient atmosphere by exposing the encapsulated devices under a 1-sun equivalent white LED irradiation. A Botest multichannel analyser system (Botest Systems GmbH, EMU-8/ v2.3) was used to maintain a constant applied voltage (initial V_{MPP}). The white light LED source (3000K Cree CXB3590) was calibrated to provide a 1 sun equivalent intensity by matching the initial current of the cell to its J_{SC} under AM1.5G illumination. The initial set temperature was room temperature, although the instrumental heating can result in rising the temperature up to ~ 37 °C.

Light/dark cycling measurements: Light/dark cycling measurements were performed using a mechanical timer connected to a white LED light source (3000 K, Cree CXB3590), which alternated between 1 hour of illumination and 1 hour of darkness. Current J-V characteristics were recorded every 30 seconds in the forward scan direction using the infinityPV MPPT tracker. All measurements were conducted inside an N_2 -filled glovebox on unencapsulated devices. The light intensity was calibrated to 1 sun equivalent by matching the initial short-circuit current density (J_{SC}) of the device to its value under AM1.5G illumination, ensuring accurate intensity alignment. Device performance parameters were extracted from the J-V curves, and the PCE was calculated accordingly. During measurements, the device temperature was maintained at 25 °C using a temperature controller. The system also allows temperature variation for temperature-dependent studies.

Long Term Photoluminescence (PL) Stability Measurements: A Alustar G2 LED from ledxon GmbH was used to illuminate the films and devices while photoluminescence (PL) spectra were recorded every minute via by OCEAN SR compact spectrometer under continuous light and light/dark cycling provided by connecting the mechanical timer to the LED. A PS-1302 D power supply from VOLTcraft was used as the power supply for LED. The measurement took place in the ambient air with encapsulated samples.

In-situ PL imaging degradation measurement: Photoluminescence (PL) degradation measurements were carried out using an Olympus BX51 microscope equipped with a cooled 2.1 MP sCMOS camera (Thorlabs CC215MU) and a motorized filter wheel containing 750 nm and 800 nm bandpass filters (40 nm FWHM). Samples were homogeneously illuminated from

below using a blue LED, while localized degradation was induced by irradiating a small area from above with a xenon (Xe) lamp. Images were acquired over time using both filters and subsequently analysed in ImageJ. Ratio images were generated by dividing the pixel-wise intensity recorded with the 800 nm filter by that obtained with the 750 nm filter.

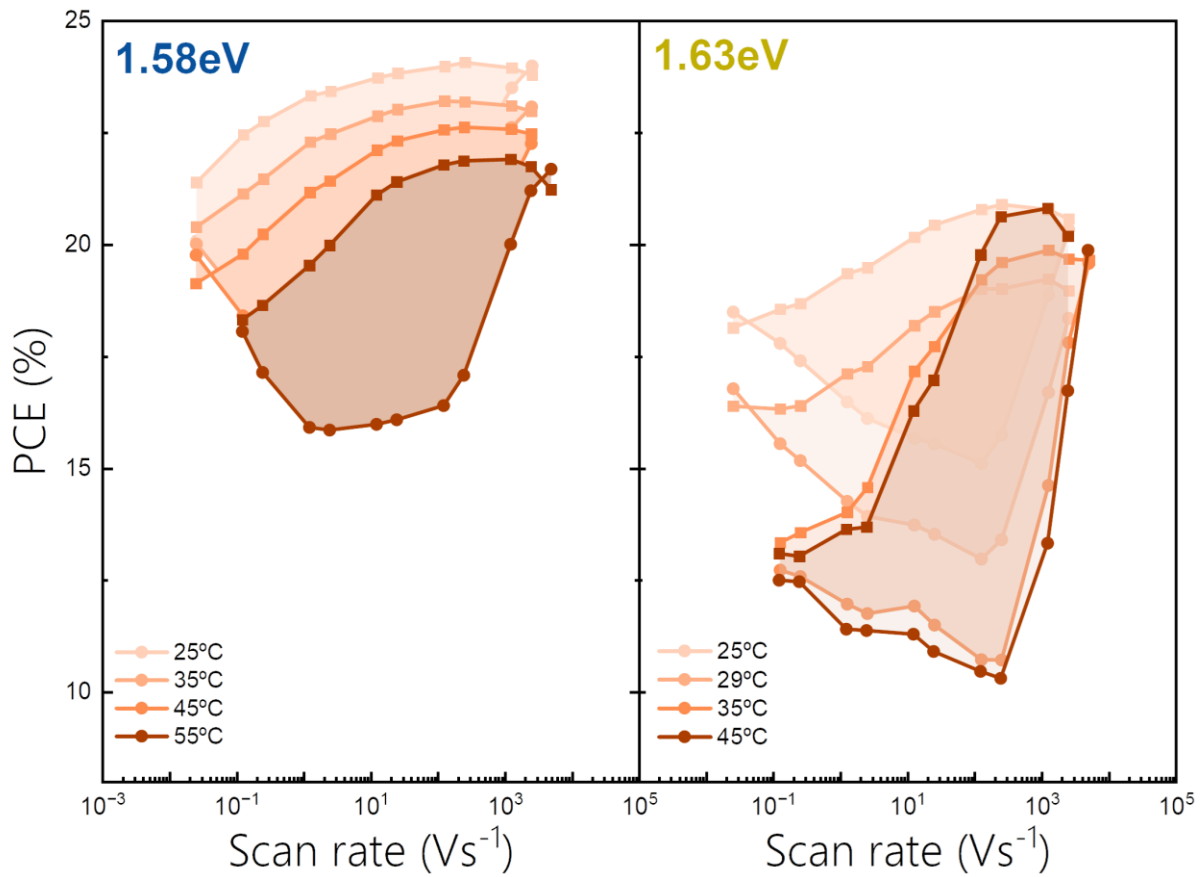


Figure S1: Temperature-dependent fast hysteresis of 1.58eV and 1.63 eV PSCs

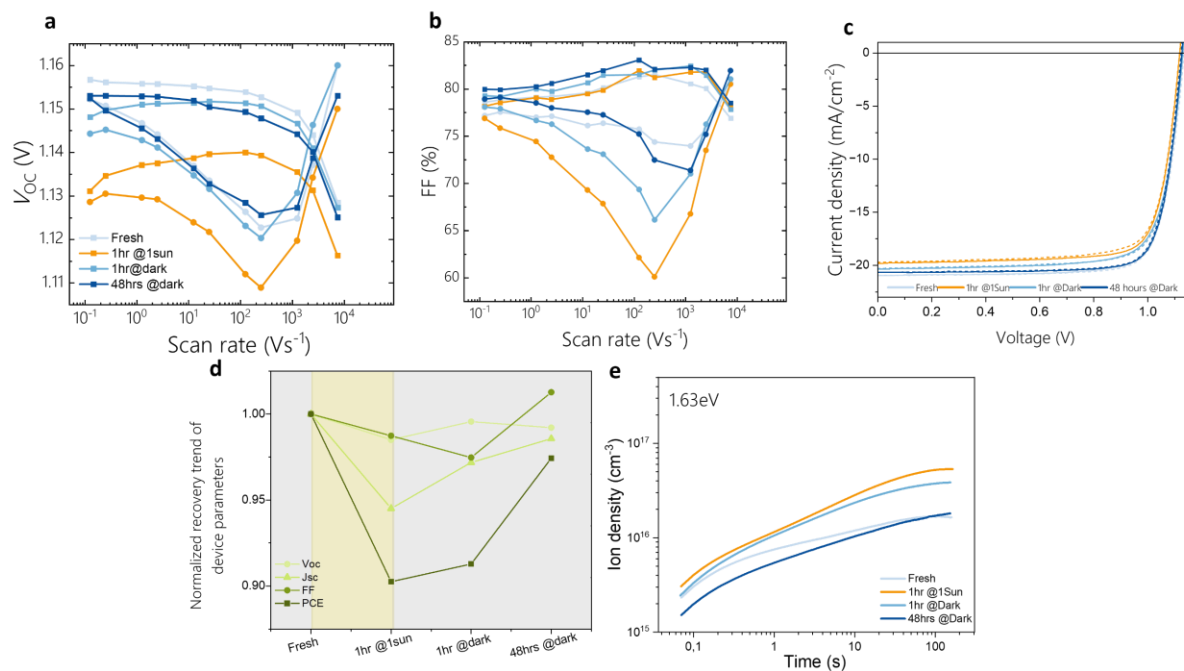


Figure S2: a) and b) V_{oc} and fill factor (FF) adopted from FH measurement at fresh, 1hour aged, 1hour recovery, and after 48 hours of recovery, c) J-V curves of 1.63eV sample at fresh, 1hour aged, 1hour recovery, and after 48 hours of recovery, d) Normalized recovery trend of device parameters at different stages of aging and recovery, e) ion density measured by BACE at different aging and recovery stages.

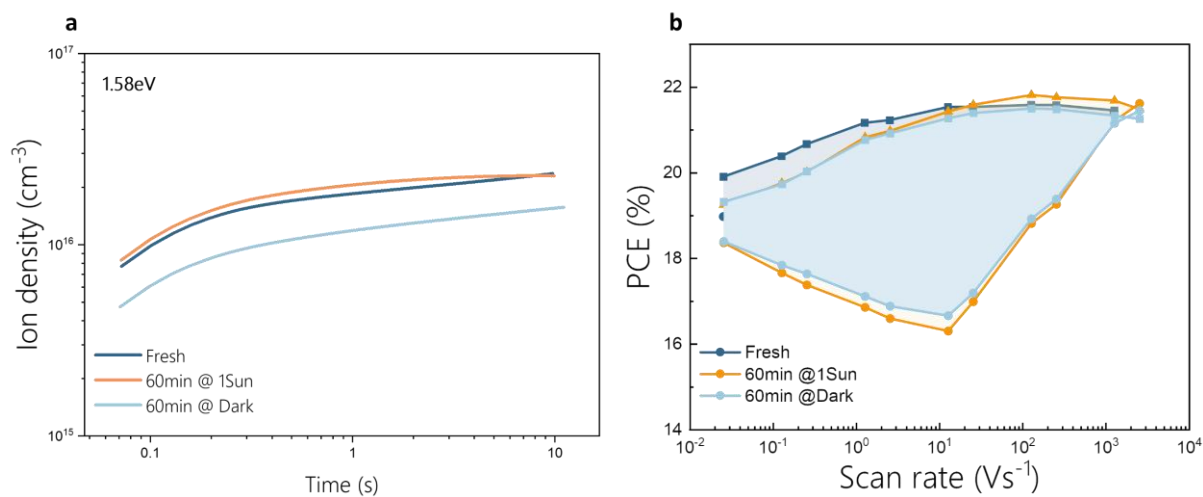


Figure S3: a) ion density measured by BACE, and b) ionic loss measured by FH for 1.58eV PSC at different aging and recovery stages.

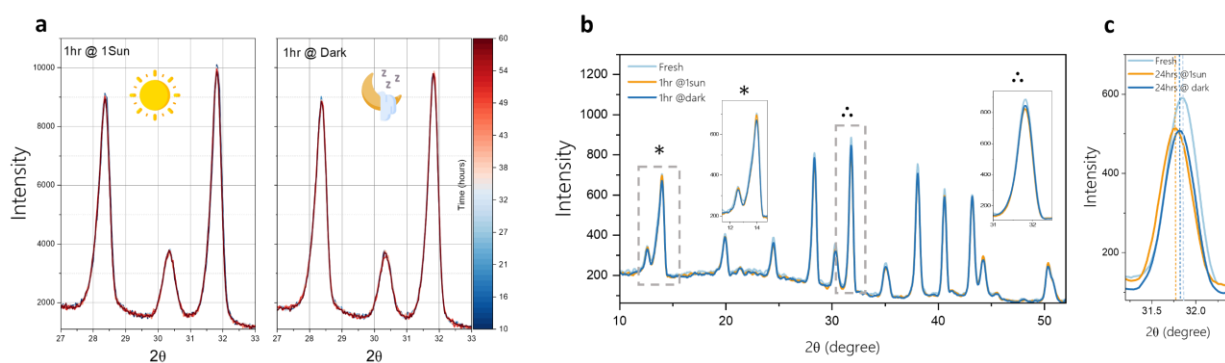


Figure S4: a) in-situ GIXRDs under 1 hour of light and 1 hour of dark resting, b) GIXRDs of the sample at fresh, after 1 hour of illumination and 1 hour of dark resting. c) GIXRD at peak 31.8 degrees after 24 hours of light and 24 hours of dark resting.

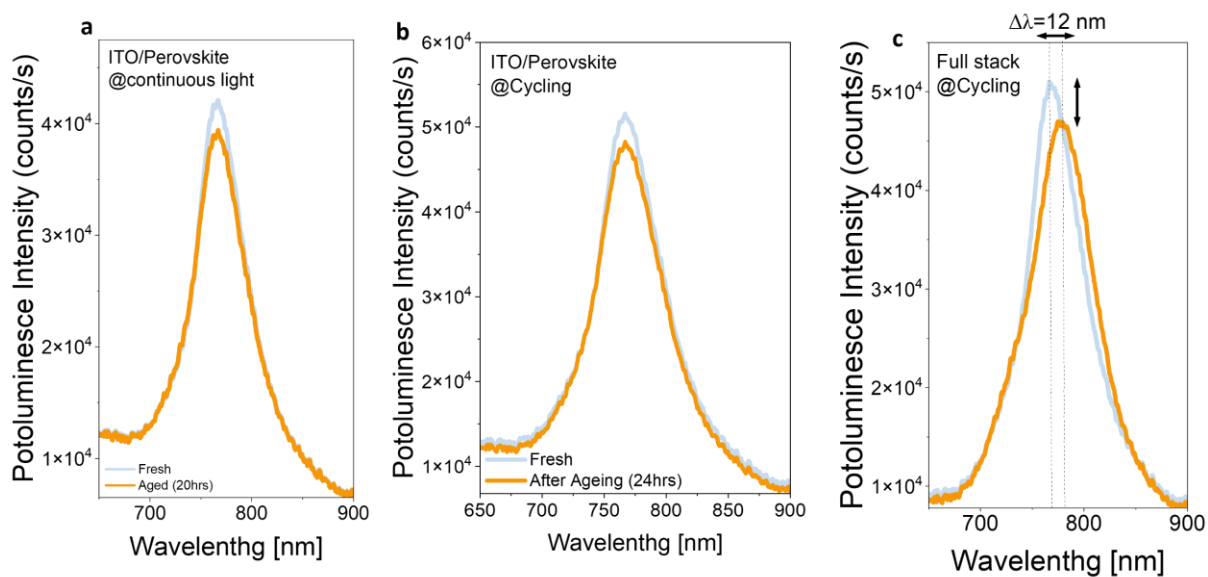


Figure S5: PL measurement of the fresh and aged for a) ITO/perovskite film under continuous light, b) ITO/perovskite film under light/dark cycling, and c) full stack under light/dark cycling.

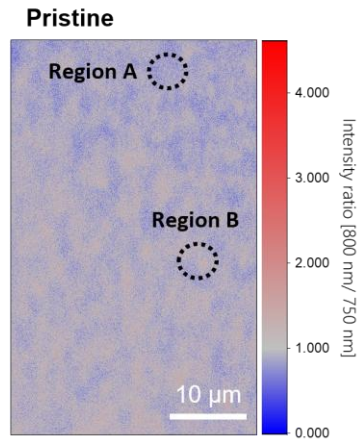


Figure S6: PL imaging for 1.63eV device at pristine stage.

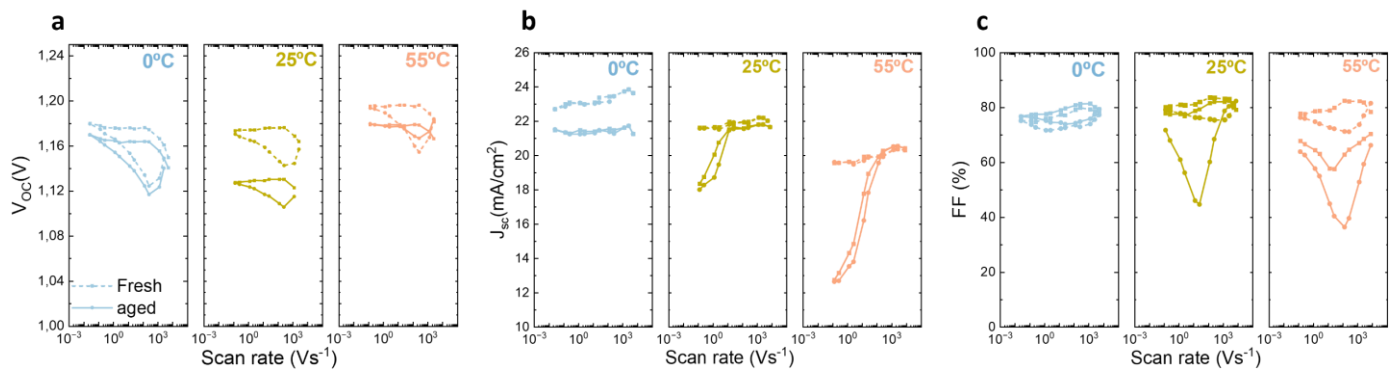


Figure S7: FH for a fresh and degraded device at different temperatures under light/dark cycling. a) V_{oc} , b) J_{sc} , c) FF for 1.63eV sample.

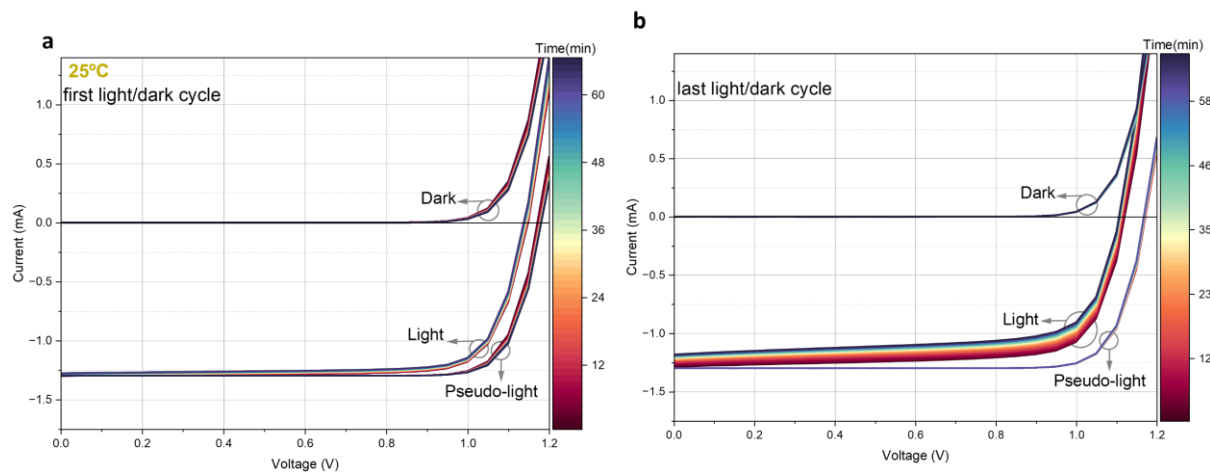


Figure S8: Deriving pseudo-light J-Vs from dark J-Vs under cycling for the 1.63 eV sample. A) for the first light/dark cycle, b) for the last light/dark cycle after 24 hrs of cycling.

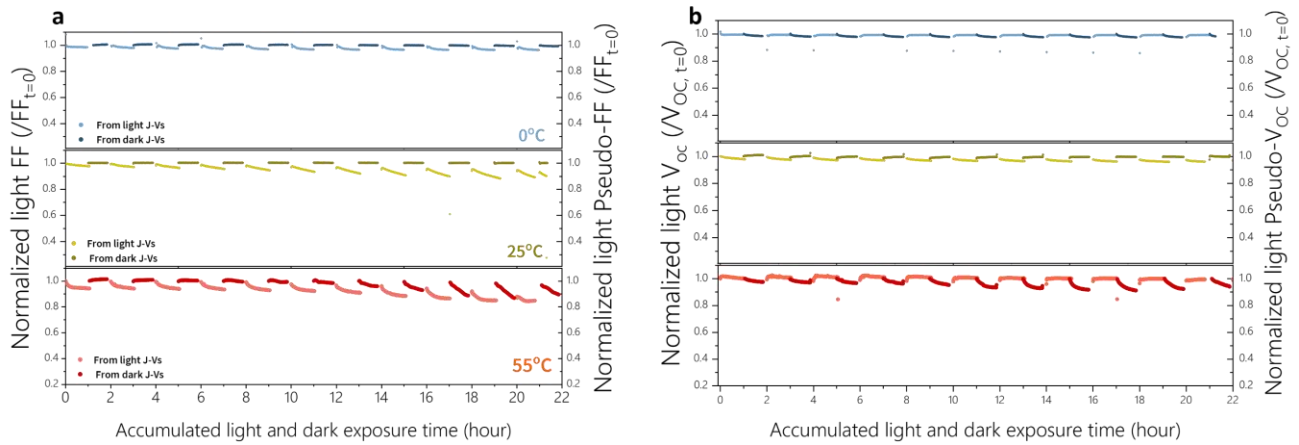


Figure S9: FF and Voc adapted from light and pseudo-dark J-Vs under 1 hour light/dark cycling at different temperatures for 1.63eV solar cell.

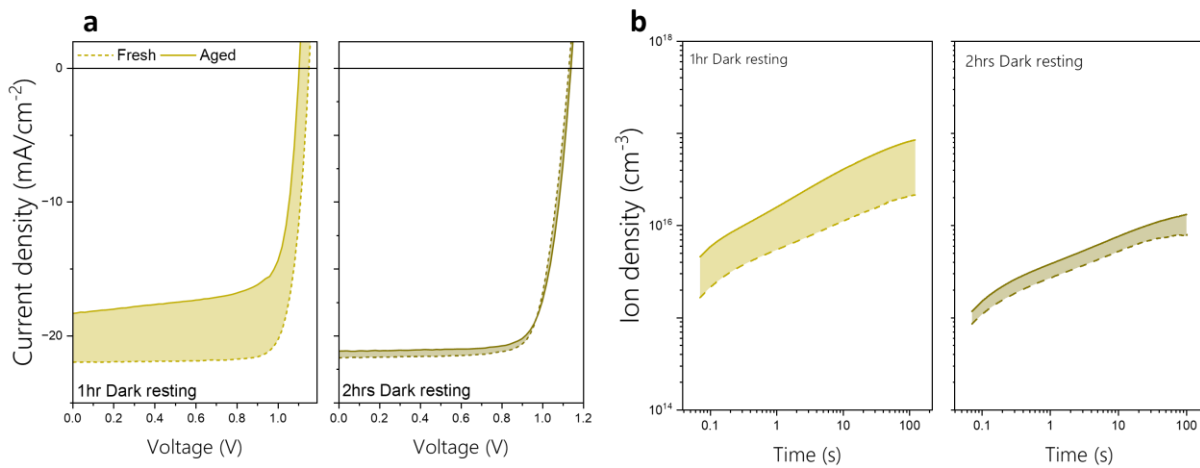


Figure 10: a) J-V and b) BACE measurement at fresh and aged samples after 12 hours for different dark periods.

References

1. Seid, B. A. *et al.* Understanding and Mitigating Atomic Oxygen-Induced Degradation of Perovskite Solar Cells for Near-Earth Space Applications. *Small* **20**, (2024).

2. Lang, F. *et al.* Influence of radiation on the properties and the stability of hybrid perovskites. *Advanced Materials* **30**, (2018).
3. Sowmeh, P. F. *et al.* Minimizing Ionic Losses in DMSO-Free Tin-Based Perovskite Solar Cells. *ACS Energy Lett.* **10**, 6215–6222 (2025).